Available online at www.sciencedirect.com
ScienceDirect
Journal of Power Sources 158 (2006) 1490–1497
JOURNAL OF POWER SOURCES
www.elsevier.com/locate/jpowsour

Modelling Ni-mH battery using Cauer and Foster structures

E. Kuhn [b], C. Forgez [b], P. Lagonotte [a], G. Friedrich [b,*]

[a] *ENSMA Laboratoire d'Etudes Thermiques, BP 40109 86961, Futuroscope Cedex, France*
[b] *Université de Technologie de Compiègne, Laboratoire d'Electromécanique, BP 20529, 60205, Compiègne, France*

Received 1 April 2005; received in revised form 26 September 2005; accepted 10 October 2005
Available online 5 December 2005

Abstract

This paper deals with dynamic models of Ni-mH battery and focuses on the development of the equivalent electric models. We propose two equivalent electric models, using Cauer and Foster structures, able to relate both dynamic and energetic behavior of the battery. These structures are well adapted to real time applications (e.g. Battery Management Systems) or system simulations. A special attention will be brought to the influence of the complexity of the equivalent electric scheme on the precision of the model. Experimental validations allow to discuss about performances of proposed models.

Keywords: Battery modelling; Nickel metal hydride; Equivalent circuit; Hybrid vehicle; Warburg impedance; Identification

1. Introduction

In the embedded electric systems, knowing the dynamic electric storage components is necessary for the optimisation of such systems. However, batteries remain the most difficult elements to model. The prediction of dynamic behaviors of batteries is essential to estimate the State of Charge (SoC) and the State of Health (SoH). Energetic flows inside the battery can be calculated using entropy variations. Such a method is dedicated to electrochemists and requires the knowledge of experimental parameters, which are not always accessible to the non-specialists [1,2]. Moreover, such methods need long time computations and cannot be implemented in processor, which are dedicated to real time applications (e.g. Battery Management Systems). Another method consists in representing battery using an equivalent electric circuit [3,4]. This method is easier to be implemented. Nevertheless, performances of the model are based on the effectiveness of the equivalent electric circuit. The circuit must be simple enough to be easily implemented in the real time applications but must be accurate enough to represent the main phenomena.

Under the linearity assumption, spectroscopy allows to represent the battery impedance in relation with frequency [5]. Most of battery equivalent electric circuits are based on spectroscopy experiments [6–9]. However, because of the nature of the diffusion phenomenon, this one remains the most difficult phenomenon to be modelled. To overcome this difficulty, some papers have proposed models based on non-integer derivatives [9–11]. Nevertheless, their development for real time applications is not trivial [12].

We propose in this paper a Ni-mH battery model using an equivalent electric circuit. The first part is dedicated to the justification of the electric component. This part focuses on the diffusion representation and we propose an analytical model. In the second part, this model is developed into Cauer and Foster structures. Identification results are presented and allow to discuss eventual order reduction. The last parts presents temporal responses to proposed models and are compared with experiments.

2. Lumped scheme

In previous works [9], we had proposed a modified Randles scheme of a Ni-mH battery. This scheme is represented Fig. 1.

This scheme relates the main static and dynamic phenomena: R_Ω stands for electrolyte and connexion resistances. The $R_{tc}C_{dl}$ parallel circuit stands for charge transfer phenomenon. In the Nyquist plot (Fig. 2), charge transfer phenomenon is defined as a semi-circle. A Warburg impedance Z_W stands for the diffusion

* Corresponding author. Tel.: +33 3 44 23 45 15; fax: +33 3 44 23 79 37.
E-mail address: guy.friedrich@utc.fr (G. Friedrich).

0378-7753/$ – see front matter © 2005 Elsevier B.V. All rights reserved.
doi:10.1016/j.jpowsour.2005.10.018

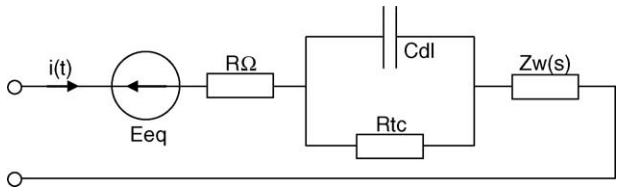

Fig. 1. Modified Randles scheme.

phenomenon which is theoretically defined as 45° slope in the Nyquist plot.

In the framework of Ni-mH battery modelling, it seems that charge transfer and diffusion phenomena occur in distinct frequency areas. Consequently, Warburg impedance appear in series with the $R_{tc}C_{dl}$ parallel circuit in the modified Randle scheme, which is not the case in the traditional Randles scheme [6]. This modification brings simplifications in the following mathematical expressions and the impedance expression becomes:

$$Z(s) = R_\Omega + \frac{R_{tc}}{1 + sR_{tc}C_{dl}} + Z_W(s) \quad (1)$$

The main difficulty of battery dynamic modelling remains the diffusion phenomenon. In the framework of a semi-infinite diffusion, Warburg impedance is theoretically expressed as a non-integer function [13].

$$Z_W(s) = \sigma\omega^{1/2}(1 - j) \quad (2)$$

where σ is a parameter which depends on the electrochemical phenomenon.

In the framework of a pure mathematical approach of the problem, we have shown that Warburg impedance could be modelled as a non-integer transfer function, the mathematical structure of which was asymptotically defined from spectroscopy experiments Bode plot [9].

The non-integer transfer function is defined as:

$$Z_W(s) = \frac{(1 + \tau_2 s)^{n_2}}{(\tau_1 s)^{n_1}} \quad (3)$$

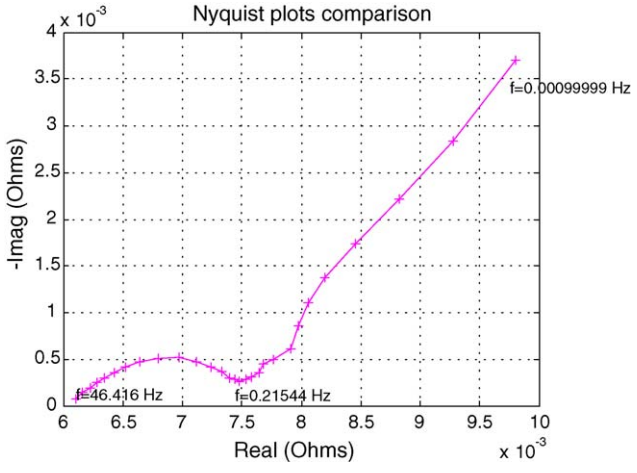

Fig. 2. Nyquist plot of a cell.

We had shown that such an expression gives good performances for the representation of the battery dynamic behavior. However, this model has two drawbacks:

- On one hand, the temporal expression of non-integer transfer function requires the knowledge of injected currents from the initial time up to the final one. This feature is due to the recursivity of diffusion phenomenon and, forbid as a consequence, the use of this model in real time applications. Nevertheless, this lack has been overcome using diffusive realisations [12].
- On the other hand, such a pure mathematical model gives a good representation of dynamic behavior but misses energetic aspects. Consequently, it does not make possible the evaluation of energetic losses inside the battery. In order to overcome this lack, we lead our research to an equivalent electric scheme of Warburg impedance, the resistive components of which could be used for the estimation of energetic losses.

The method consists in developing an analytical model of Warburg impedance in functions series, and identifying this development with an equivalent impedance composed of capacities and resistances.

The used analytical model of Warburg impedance is an hyperbolic tangent one. This model has already been proposed in previous works [7]:

$$Z_W(s) = \frac{k_2}{\sqrt{s}} \tan h\left(\frac{k_1}{k_2}\sqrt{s}\right) \quad (4)$$

The two following sections are dedicated to the development of this model into electric equivalent structures.

3. Development in serie of Warburg impedance

3.1. Mittag-Leffler's theorem

Mittag-Leffler theorem can be considered as a generalisation, to the meromorphic functions, of partial fraction decomposition. All complex rational fractions can be decomposed into a sum of first order elements. Particularly, if a rational function P/Q has no simple pole p_n, $1 \le n \le N$, P/Q can be written as:

$$\frac{P(x)}{Q(x)} = A(x) + \sum_{n=1}^{N} \frac{a_n}{(x - p_n)} \quad (5)$$

where A is a polyoma and a_n is the residue corresponding to the pole p_n.

Let us consider a meromorphic function f with only simple poles p_n ordered to increasing modulus. If a serie of circles C_n, with the radius R_n, exists in the complex plane, independent of any pole of function f, $|f(x)| < M$, M is independent of n so that $\mathrm{Rn} \to \infty$ when $n \to \infty$, then Mittag-Leffler's theorem give the following decomposition:

$$f(x) = f(0) + \sum_{n=1}^{\infty} a_n \left(\frac{1}{x + p_n} + \frac{1}{p_n}\right) \quad (6)$$

Hyperbolic tangent verifies theorem and can be decomposed following an infinite number of imaginary poles

$$p_n = j\left(n\pi - \frac{\pi}{2}\right) \tag{7}$$

After simplifications, hyperbolic tangent can be written as a series of function

$$\tan h(x) = \sum_{n=-\infty}^{\infty} \frac{1}{x - j\left(n\pi - \frac{\pi}{2}\right)} \tag{8}$$

Using properties of complex conjugate poles, the series can be rewritten as:

$$\tan h(x) = \sum_{n=1}^{\infty} \frac{2x}{x^2 + \left(n\pi - \frac{\pi}{2}\right)^2} \tag{9}$$

3.2. Foster structure

Hyperbolic tangent used to model Warburg impedance can be decomposed using Mittag-Leffler's theorem.

$$Z_W(s) = \frac{k_2}{\sqrt{s}} \sum_{n=1}^{\infty} \frac{\frac{2k_1\sqrt{s}}{k_2}}{\left(\frac{k_1}{k_2}\right)^2 s + \left(n\pi - \frac{\pi}{2}\right)^2} \tag{10}$$

This expression can be simplified:

$$Z_W(s) = \sum_{n=1}^{\infty} \frac{1}{\frac{k_1}{2k_2^2}s + \frac{1}{2k_1}\left(n\pi - \frac{\pi}{2}\right)^2} \tag{11}$$

The series of function can be identified as a series of cells made of admittance and impedance.

$$Z_W(s) = \sum_{n=1}^{\infty} \frac{1}{Y_n + \frac{1}{Z_n}} \tag{12}$$

By limiting the development to the $2n$ main poles, we get a finite Foster network synthesis Fig. 3 [14,15].

The values of the components can be deduced by identification:

$$Z_n = \frac{2k_1}{\left(n\pi - \frac{\pi}{2}\right)^2}; \qquad Y_n = \frac{k_1}{2k_2^2}s \tag{13}$$

Consequently, the admittances Y_n denote capacities and impedances Z_n denote resistances so that:

$$R_n = \frac{8k_1}{(2n-1)^2\pi^2}; \qquad C_n = \frac{k_1}{2k_2^2} \tag{14}$$

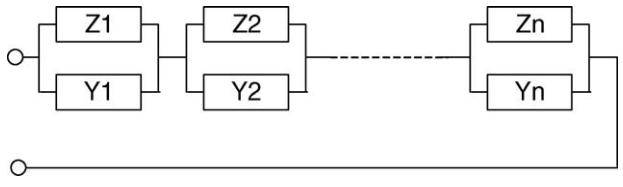

Fig. 3. Reduced order model for Z_w.

3.3. Development into continued fractions

Nowadays, developments into continued fractions are still used to get rational approximations for numerical solving of complex problems, especially in theoretical physical domain. The French mathematician H. Padè (1863–1953) gave his name to a class of such approximations, which were formalized by Lagrange and Lambert's works. Padé approximation is a partial fraction P/Q, the development of which fits as best as possible the f function to be approximated, so that [16]:

$$Q(x)f(x) - P(x) = O(x^{m+n+1}) \tag{15}$$

where P and Q are polynomials, the degrees of which are respectively equal or inferior to m and n. If such polynomials exist, they define a unique partial fraction called Padé approximation.

Let us consider the development in series of hyperbolic tangent:

$$\tan h(x) = x - \frac{1}{3}x^3 + \frac{2}{15}x^5 + \cdots \tag{16}$$

or

$$\tan h(x) = \frac{1}{\frac{1}{x - \frac{1}{3}x^3 + \frac{2}{15}x^5 + \cdots}} \tag{17}$$

The inverse of hyperbolic tangent can be developed in Laurent series:

$$\frac{1}{x - \frac{1}{3}x^3 + \frac{2}{15}x^5 + \cdots} = \frac{1}{x} + \frac{x}{3} - \frac{x^3}{45} + \cdots \tag{18}$$

By using this development in the previous expression we get:

$$\tan h(x) = \frac{1}{\frac{1}{x} + \frac{1}{\frac{3}{x} + \frac{x}{5} + \frac{x^3}{175} + \ldots}} \tag{19}$$

By repeating the development into Laurent series of residues we get a development into continued fractions of hyperbolic tangent.

$$\tan h(x) = \frac{1}{\frac{1}{x} + \frac{1}{\frac{3}{x} + \frac{1}{\frac{5}{x} + \frac{1}{\frac{7}{x} + \cdots}}}} \tag{20}$$

3.4. Cauer structure

The development into continued fractions of our model of Warburg impedance leads to:

$$\frac{k_2}{\sqrt{s}} \tan h\left(\frac{k_1}{k_2}\sqrt{s}\right) = \frac{k_2}{\sqrt{s}} \frac{1}{\frac{1}{\frac{k_1}{k_2}\sqrt{s}} + \frac{1}{\frac{3}{\frac{k_1}{k_2}\sqrt{s}} + \frac{1}{\frac{5}{\frac{k_1}{k_2}\sqrt{s}} + \frac{1}{\frac{7}{\frac{k_1}{k_2}\sqrt{s}} + \cdots}}}} \tag{21}$$

after simplification we get:

$$Z_W(s) = \frac{1}{\frac{1}{k_1} + \frac{1}{\frac{3k_2^2}{k_1 s} + \frac{1}{\frac{5}{k_1} + \frac{1}{\frac{7k_2^2}{k_1 s} + \cdots}}}} \tag{22}$$

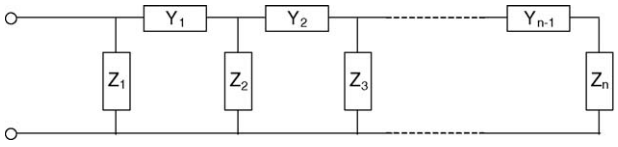

Fig. 4. Reduced order model for Z_w.

This expression can be identified in relation with the following impedance:

$$Z_W(s) = \cfrac{1}{\frac{1}{Z_1} + \cfrac{1}{\frac{1}{Y_1} + \cfrac{1}{\frac{1}{Z_2} + \cfrac{1}{\frac{1}{Y_2} + \cdots}}}} \tag{23}$$

with

$$Z_n = \frac{k_1}{4n-3}; \qquad Y_n = \frac{k_1 s}{k_2^2(4n-1)} \tag{24}$$

Consequently, the admittances Y_n denote capacities and impedances Z_n denote resistances so that:

$$R_n = \frac{k_1}{4n-3}; \qquad C_n = \frac{k_1}{k_2^2(4n-1)} \tag{25}$$

The corresponding equivalent electric circuit is presented as a Cauer network synthesis Fig. 4 [17].

4. Identification

4.1. Initialisation and identification process

We have shown in the previous parts how we obtained from development of an analytical model two equivalent electric circuits. Foster structure has been deduced from development based on Mittag-Leffler theorem, and Cauer structure has been deduced from development based on continued fractions. In order to prevent time calculation expansion, in the framework of a real time implementation of the model, we have limited the number of *RC* cells corresponding to the Warburg impedance model. In a first step, we fixed the number to four cells. The corresponding equivalent electric structures are presented Figs. 5 and 6.

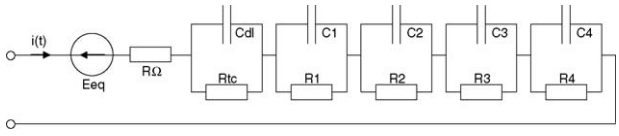

Fig. 5. Reduced order model using Foster structure.

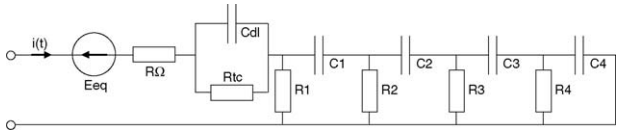

Fig. 6. Reduced order model using Cauer structure.

Each component of the structures must be identified in order to approximate as best as possible spectroscopy experiments on a wide frequency range (10^{-3} Hz up to 46 Hz) and for states of charge 60%, 80% and 99%. These states of charge correspond to the range where batteries traditionally operate in electric hybrid vehicle.

Identification process consists in minimizing least square errors of real and imaginary parts between actual and estimated impedances. This well known method is called complex non-linear least squares method [18]. In a first step we use Eq. (1) in which we identified the parameters R_Ω, R_{tc}, C_{dl}, K_1, K_2. Then, parameters k_1 and k_2 are used to set up parameters of Foster and Cauer structures according to Eqs. (14) and (25).

Nyquist plots show clearly the semi-circle, which represents the charge transfer phenomenon and 45° slope, which represents diffusion phenomenon.

We have represented in Fig. 7 and Table 1 identification results of Cauer and Foster structures with four cells set up using Eqs. (14) and (25).

We can see that model fits very well the charge transfer phenomena (semi-circle feature). As regards the diffusion phenomena, we can see that the modelling is not perfect. Indeed, the slope represented by the two models does not correspond exactly to the actual slope. Moreover, models loose precision in the very low frequencies. We can also notice a difference between the slopes of the models.

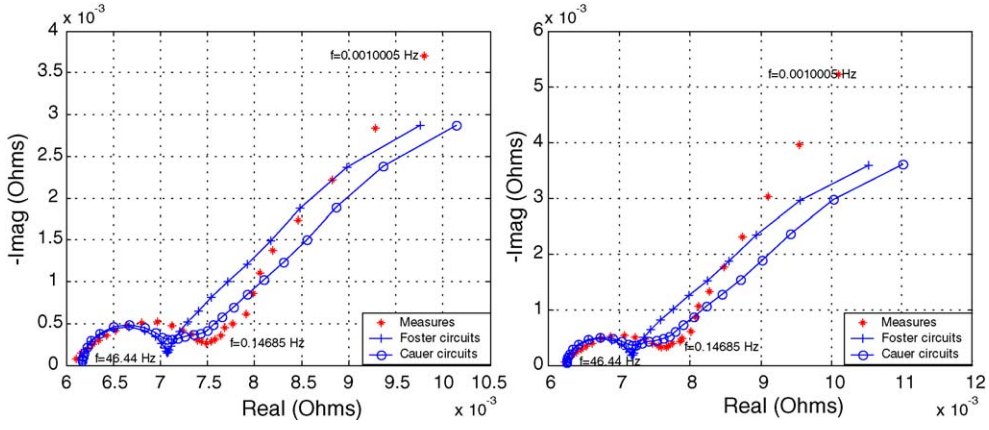

Fig. 7. Nyquist plots at SoC 60% and 99% with four cells.

Table 1
Values of components for the Cauer and Foster structure (four cells)

	SoC 60 ($k_1 = 7.6 \times 10^{-3}$, $k_2 = 2.98 \times 10^{-4}$)		SoC 80 ($k_1 = 7.5 \times 10^{-3}$, $k_2 = 3.01 \times 10^{-4}$)		SoC 99 ($k_1 = 9.55 \times 10^{-3}$, $k_2 = 3.73 \times 10^{-4}$)	
	Cauer	Foster	Cauer	Foster	Cauer	Foster
R_Ω (mΩ)	6.17	6.17	6.21	6.21	6.25	6.25
R_{tc} (mΩ)	0.91	0.91	0.96	0.96	0.93	0.93
C_{di} (F)	73.31	73.31	75.25	75.25	77.7	77.7
R_1 (mΩ)	7.6	6.16	7.5	6.07	9.5	7.7
C_1 (F)	28527	42791	27575	41363	22880	34321
R_2 (mΩ)	1.52	0.68	1.5	0.67	1.9	0.86
C_2 (F)	12226	42791	11818	41363	9805	34321
R_3 (mΩ)	0.84	0.24	0.83	0.24	1.06	0.30
C_3 (F)	7.78	42791	7520	41363	6240	34321
R_4 (mΩ)	0.58	0.12	0.57	0.12	0.73	0.15
C_4 (F)	5705	42791	5515	41363	4576	34321

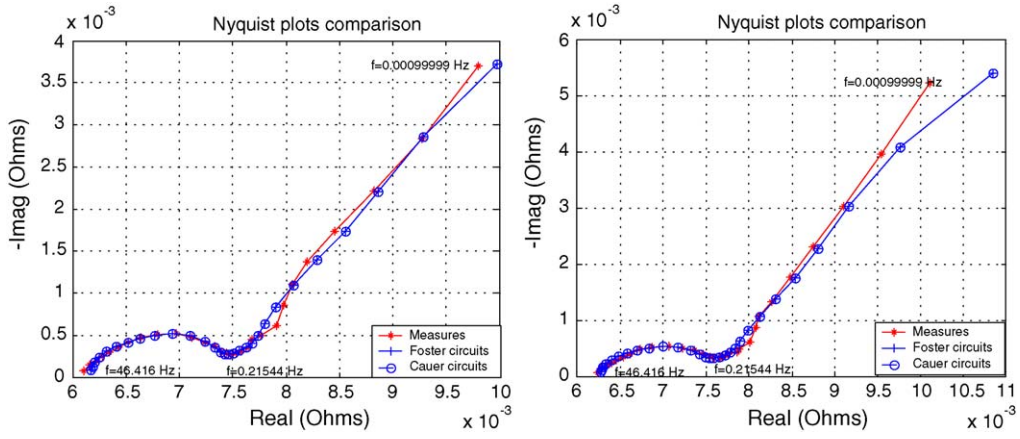

Fig. 8. Nyquist plots at SoC 60% and 99% with enhanced parameters (four cells).

4.2. Enhanced model

In order to get a better fitting, we use the previous identification results as a set up for parameters structures on which we are repeating the complex non-linear least squares method.

The parameters set becomes R_Ω, R_{tc}, C_{dl}, R_1, C_1, R_2, C_2, . . ., R_n, C_n. The increase of parameters number (in our case 11 elements instead of five in the previous part) allow to increase the number of degrees of freedom which offer a finest approach of spectroscopy experiments.

Fig. 8 and Table 2 present identification results with these parameters improvement.

With this identification process and parameter refinement, the Cauer and Foster structure give the same results and fit very well both charge transfer and diffusion phenomena on the whole range of spectroscopy experiments.

Table 2
Optimised values of components for the Cauer and Foster structure (four cells)

	Cauer			Foster		
	SoC 60%	SoC 80%	SoC 99%	SoC 60%	SoC 80%	SoC 99%
R_Ω (mΩ)	6.17	6.21	6.25	6.17	6.21	6.25
R_{tc} (mΩ)	0.41	0.49	0.39	0.41	0.49	0.39
C_{dl} (F)	52.8	54.3	60.5	52.8	54.6	60.6
R_1 (mΩ)	13.1	20.9	17.1	10.95	18.2	15
C_1 (F)	28187	30812	20165	40203	40164	26000
R_2 (mΩ)	2.38	2.65	2.21	1.04	1.37	0.88
C_2 (F)	7857	18287	5262	33724	67286	28078
R_3 (mΩ)	2.372	2.56	2.64	0.29	0.49	0.32
C_3 (F)	618	2187	519	836	15336	6054
R_4 (mΩ)	2.42	2.20	2.12	0.84	0.83	0.86
C_4 (F)	188	208	209	144	191	149

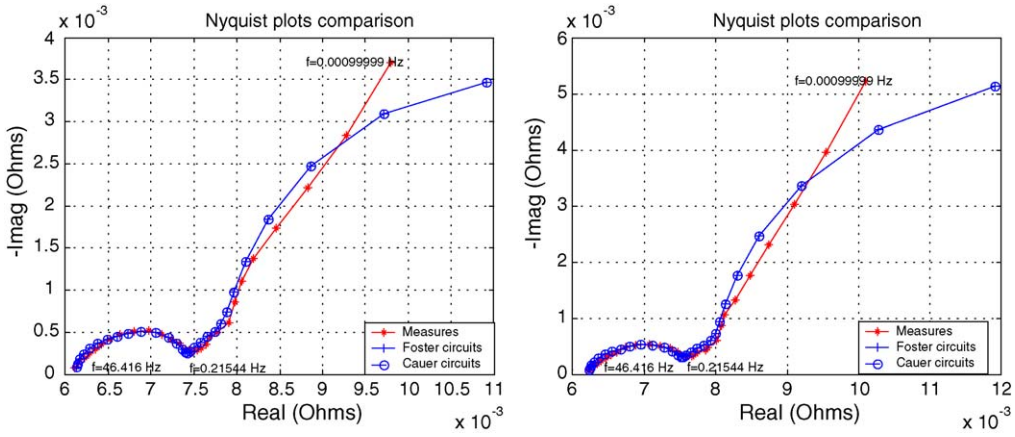

Fig. 9. Nyquist plots at SoC 60% and 99% with enhanced parameters (three cells).

4.3. Reduced order model

Keeping in mind the possibility to implement the battery model in a real time application, we wanted to reduce the order of the model. Consequently, we have reduced to three *RC* cells, the equivalent circuit of Warburg impedance in the two structures. The identification process is the same as in the previous section. Fig. 9 and Table 3 present the corresponding identification results. The order reduction of the model damages the quality of diffusion approximation. The choice of four *RC* cells to model diffusion phenomenon seems to be the best trade off in our application. We are going to validate time responses of the three and four cells structures in order to verify the performances.

5. Current steps validations

In the previous section, we have presented spectroscopy experiments and model of one element of our battery. This one is made of 32 elements 1.2 V 13.5 A h in series. Consequently, under the assumption of homogeneous behavior of the 32 elements, we have considered the model of our battery as 32 times the model of one element. In the following sections, we present comparisons between experimental and simulation results of current steps responses. The current steps have been imposed to the battery thanks to a linear amplifier.

5.1. Short current steps validations

We have imposed current sollicitations to our battery. Figs. 10 and 11 present voltage variations, around equilibrium voltage, of experimental and simulation results when we imposed $\frac{-C}{3}$ up to $\frac{C}{3}$ current steps. We can see that the structures with three or four cells give similar responses and are very close from actual battery response.

These good results can be explained because fundamental frequency of current steps (0.5 Hz) is relatively high and corresponds to charge transfer frequencies range (Fig. 2). In this area (semi-circle), the structures with three or four cells model perfectly spectroscopy experiments Figs. 8 and 9.

5.2. Long current steps validations

We have also validated steady current steps by imposing a $\frac{C}{3}$ constant current during 1000 s. Results of Fig. 12 show the divergence between model and battery responses of voltage variations around equilibrium voltage. The difference is, all the more important for the structure with three cells because of the bad approximation of this structure in the very low frequencies.

These validations show the difficulty to model the dynamic behavior of the battery in a wide range of frequencies and focuses on the importance of the model structure.

Table 3
Values of components for the Cauer and Foster structure (three cells)

	Cauer			Foster		
	SoC 60%	SoC 80%	SoC 99%	SoC 60%	SoC 80%	SoC 99%
R_Ω (mΩ)	6.17	6.21	6.25	6.17	6.21	6.25
R_{tc} (mΩ)	0.46	0.49	0.45	0.46	0.49	0.45
C_{dl} (F)	50.8	54.5	57.8	50.8	54.5	57.8
R_{tc} (mΩ)	8.2	11.5	11.9	6.95	10.2	10.6
C_1 (F)	18553	21127	15527	25931	27140	19706
R_2 (mΩ)	1.47	1.5	1.5	0.82	0.82	0.49
C_2 (F)	1403	2473	1170	169	194	8152
R_3 (mΩ)	2.03	1.92	1.93	0.45	0.54	0.85
C_3 (F)	189	208	201	10728	15120	174

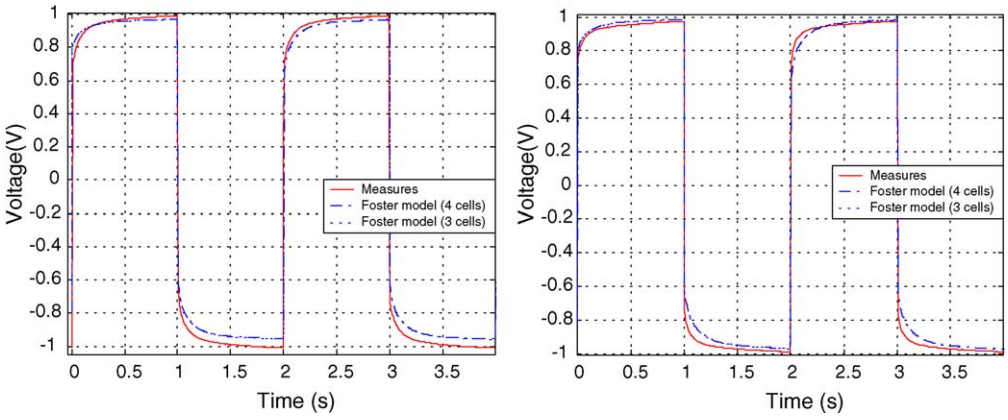

Fig. 10. Alternative step responses at SoC 60% and 99%.

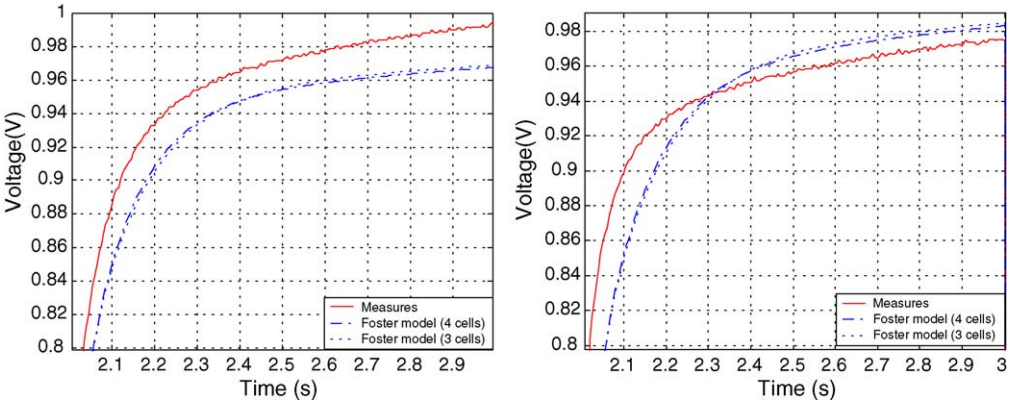

Fig. 11. Zoom of alternative step responses at Soc 60% and 99%.

However, it is necessary to relativize the extrapolation in the very low frequencies or in steady state. On one hand, we have no information about battery impedance in this frequency range, and on another hand, the notion of dynamic impedance in this frequency range has no significant sense. Indeed, at very low frequency or in steady states, it is not possible to obtain correct spectroscopy experiments because the state of charge changes significantly when measuring and consequently, parameters change also in the same way. In this area, Nyquist plot at a given state of charge has no more sense.

6. Conclusion

We have presented in this paper two equivalent electric circuits to model the dynamic behavior of a Ni-mH battery. The proposed Cauer and Foster structures made possible the modelling of the diffusion phenomenon using a finite network of capacities and resistances despite the recursive nature of this phenomenon. We have shown that developments into Cauer or Foster structures have given similar results in condition to refine the identification process on the whole parameters. We attempted

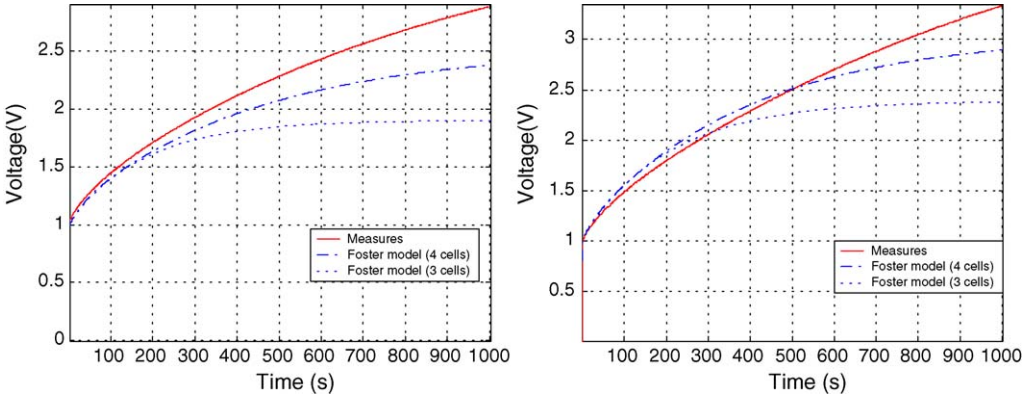

Fig. 12. Long step responses at SoC 60% and 99%.

to reduce the order of the model in order to make a real time implementation of such a model for an embedded applications like a battery management system easier. In this framework, we have shown that four cells to model diffusion phenomenon was the best trade off between performance and complexity. Finally, we have established the validity limits in a frequency range of such a dynamic model.

References

[1] J. Horno, M. Garcia-Hernandez, Digital simulation of electrochemical process by the network approach, J. Electroanal. Chem. 352 (1993) 83–97.

[2] M. Viitanen, A mathematical model for metal hydride electrodes, J. Electrochem. Soc. 140 (4) (1993) 936–942.

[3] P. Notten, Electronic-network modelling of rechargeable Ni–Cd cells and its application to the design of battery management systems, J. Power Sources 77 (2000) 143–158.

[4] T. Brumleve, Transmission line equivalent circuit models for electrochemical impedances, J. Electroanal. Chem. 126 (1981) 73–104.

[5] F. Huet, A review of impedance measurements for determination of the state of charge or state of health of secondary batteries, J. Power Sources 87 (2000) 12–20.

[6] A. Bard, Electrochemical Methods, Fundamental and Applications, 2nd ed., Wiley, 2000.

[7] P. Mauracher, E. Karden, Dynamic modelling of lead/acid batteries using impedance spectroscopy for parameter identification, J. Power Sources 67 (1997) 69–84.

[8] M. Ceraolo, New dynamical models of lead-acid batteries, IEEE Trans. Power Syst. 15 (4) (2000) 1184–1190.

[9] E. Kuhn, C. Forgez, G. Friedrich, Modelling diffusive phenomena using non-integer derivatives: application Ni-mH batteries, Eur. Phys. J. Appl. Phys. 25 (2004) 183–190.

[10] A.L. Méhauté, G. Crepy, Introduction to transfer and motion in fractal media: the geometry of kinetics, Solid State Ionics 9 (1983) 17–30.

[11] G. Fruchter, G. Crepy, A.L. Méhauté, Batteries, identified fractal objects, J. Power Sources 18 (1986) 51–62.

[12] E. Kuhn, C. Forgez, G. Friedrich, Fractional and diffusive representation of a 42 V Ni-mH battery, Fractional derivatives and their applications Ubooks, 2005, 423–434.

[13] D. Landolt, Corrosion et chimie de surfaces des métaux, Traité des matériaux, Presses Polytechniques et Universitaires Romandes, 1993.

[14] R. Foster, A reactance theorem, Bell Syst. Tech. J. 3 (1924a) 259–267.

[15] R. Foster, Theorems regarding the driving point impedance of two mesh circuits, Bell Syst. Tech. J. 3 (1924b) 651–685.

[16] A. Baker, J. Gammel, J. George, The Padé Approximant in Theorical Physics, Mathematic in Science and Engineering, Academic Press, New York, 1970.

[17] W. Cauer, Die Verwirkhchung von Wechselstromwiderständen vorgeschriebener Frequenzabhängigkeit, Archiv für Elektrotechnik 17 (1926) 355–388.

[18] J. Macdonald, Impedance Spectroscopy, Wiley-Interscience, 1987.